PHYSICAL REVIEW D **77,** 074017 (2008)

Chiral transitions in heavy-light mesons

A. M. Badalian,* Yu. A. Simonov,† and M. A. Trusov‡

ITEP, Bol'shaya Cheremushkinskaya Street 25, Moscow, Russia

(Received 30 December 2007; published 24 April 2008)

The mass shifts of the P-wave D_s and B_s mesons due to coupling to DK, D^*K and BK, B^*K channels are studied using the chiral quark-pion Lagrangian not containing fitting parameters. The large mass shifts down ~ 140 MeV and ~ 100 MeV for $D_s^*(0^+)$ and $D_s(1^{+'})$ and ~ 100 MeV for $B_s^*(0^+)$ and $B_s(1^{+'})$ are calculated. Two factors are essential for large mass shifts: strong coupling of the 0^+ and $1^{+'}$ states to the S-wave decay channel, containing a Nambu-Goldstone meson, and the chiral flip transitions due to the bispinor structure of both heavy-light mesons. The masses $M(B_s^*(0^+)) = 5710(15)$ MeV and $M(B_s(1^{+'})) = 5730(15)$ MeV, very close to $M(B(0^+))$ and $M(B(1^{+'}))$, are predicted. The experimental limit on the width $\Gamma(D_{s1}(2536)) < 2.3$ MeV puts strong restrictions on the admissible mixing angle between the 1^+ and $1^{+'}$ states, $|\phi| < 6°$, which corresponds to the mixing angle θ between the $^3P_1$ and $^1P_1$ states, $29° < \theta < 41°$.

DOI: 10.1103/PhysRevD.77.074017 PACS numbers: 14.40.Lb, 12.39.Fe, 12.40.Yx, 14.40.Nd

I. INTRODUCTION

The heavy-light (HL) mesons play a special role in hadron spectroscopy. First of all, a HL meson is the simplest system, containing one light quark in the field of almost static heavy antiquark, and it allows one to study quark (meson) chiral properties. The discovery of the $D_s(2317)$ and $D_s(2460)$ mesons [1,2] with surprisingly small widths and low masses has given us an important impetus to study chiral dynamics, and raised the question of why their masses are considerably lower than the expected values in single-channel potential models. The question has been studied in different approaches: in relativistic quark model calculations [3–6], on the lattice [7], in QCD sum rules [8,9], and in chiral models [10–12] (for reviews see also [13,14]). The masses of $D_s(0^+)$ and $D_s(1^{+'})$ in closed-channel approximation typically exceed their experimental numbers by ~ 140 and 90 MeV.

Thus the main theoretical goal is to understand the dynamical mechanism responsible for such large mass shifts of the 0^+ and $1^{+'}$ levels (both states have the light-quark orbital angular momentum $l = 0$ and $j = 1/2$) and explain why the position of the other two levels (with $j = 3/2$) remains practically unchanged. The importance of the second fact has been underlined by S. Godfrey in [5].

The mass shifts of the $D_s(0^+, 1^{+'})$ mesons have already been considered in a number of papers with the use of the unitarized coupled-channel model [15], the nonrelativistic Cornell model [16], and different chiral models [17–19]. Here we address again this problem with the aim of also calculating the mass shifts of the $D_s(1^{+'})$ and $B_s(0^+, 1^{+'})$ states and the widths of the 2^+ and 1^+ states, following the approach developed in [18], for which strong coupling to the S-wave decay channel, containing a pseudoscalar (P) Nambu-Goldstone (NG) meson, is crucially important. Therefore, in this approach the principal difference exists between vector-vector (VV) and VP (or PP) channels. This analysis of two-channel systems is performed with the use of the chiral quark-pion Lagrangian which has been derived directly from the QCD Lagrangian [20] and does not contain fitting parameters, so that the shift of the $D_s^*(0^+)$ state ~ 140 MeV is only determined by the conventional decay constant f_K.

Here the term "chiral dynamics" implies the mechanism by which, in the transition from one HL meson to another, the octet of the NG mesons ϕ is emitted. The corresponding Lagrangian $\Delta L_{\rm FCM}$,

$$\Delta L_{\rm FCM} = \bar{q}(\sigma r)\exp(i\gamma_5\phi/f_\pi)q, \tag{1}$$

contains the light-quark part, $\exp(i\gamma_5\phi/f_\pi)$, where ϕ is the $SU(3)$ octet of NG mesons and the important factor γ_5 is present. In the lowest order in ϕ this Lagrangian coincides with the well-known effective Lagrangian $\Delta L_{\rm eff}$ suggested in [21,22], where, however, an arbitrary constant g_A is introduced. At large N_c, as argued in [21], this constant has to be equal to unity, $g_A = 1$. In [10,17,22] this effective Lagrangian was applied to describe decays of HL mesons taking $g_A < 0.80$.

A more general Lagrangian $\Delta L_{\rm FCM}$ (1) was derived in the framework of the field correlator method (FCM) [20,23], in which the constant $g_A = 1$ in all cases, and which contains NG mesons to all orders, as seen from its explicit expression (1).

In Appendix A with the use of the Dirac equation we show that in the lowest order in ϕ $\Delta L_{\rm FCM} = \Delta L_{\rm eff}$, if indeed $g_A = 1$. In our calculations we always use $\Delta L_{\rm FCM}$ with $g_A = 1$ and derive the nonlinear equation for the energy shift and width, $\Delta E = \Delta\bar{E} - \frac{i\Gamma}{2}$, as in [18]. We do not assume any chiral dynamics for the unperturbed levels, which are calculated here with the use of the QCD string Hamiltonian [24,25], because the mass shift ΔE

*badalian@itep.ru
†simonov@itep.ru
‡trusov@itep.ru

appears to be weakly dependent on the position of the unperturbed level. Nevertheless, the uncertainty in the final mass values is due to a poor knowledge of the fine-structure (FS) interaction in the initial (unperturbed) P-wave masses.

It is essential that the resulting shifts of the $J^P(0^+, 1^{+'})$ levels are large only for the D_s, B_s mesons, which lie close to the DK, D^*K, BK, B^*K thresholds, but not for the $D(1P)$, $B(1P)$ mesons, in this way violating symmetry between them (this symmetry is possible in the closed-channel approximation). In our calculations, shifted masses of the $D_s(0^+)$ and $B_s(0^+)$ practically coincide with those for the $D(0^+)$ and $B(0^+)$, in agreement with the experimental fact that $M_{\rm exp}(D(0^+)) = 2350 \pm 50$ MeV [26] is equal or even larger than $M_{\rm exp}(D_s(0^+)) = 2317$ MeV. The states with $j = 3/2 D_s(1^+, 2^+)$ and $D(1^+, 2^+)$ have no mass shifts, and for them the mass difference is $\sim$100 MeV, which just corresponds to the mass difference between the s- and light-quark dynamical masses.

For the $D_s(1^{+'})$ and $B_s(1^{+'})$ mesons, the calculated masses are also close to those of the D and B mesons. Therefore, for given chiral dynamics the $J^P(0^+, 1^{+'})$ states cannot be considered as the chiral partners of the ground-state multiplet $J^P(0^-, 1^-)$, as suggested in [11].

We also analyze why two other members of the $1P$ multiplet, with $J^P = 2^+$ and 1^+, do not acquire the mass shifts due to decay channel coupling (DCC) and have small widths. Such a situation occurs if the states 1^+ and $1^{+'}$ appear to be almost pure $j = \frac{3}{2}$ and $j = \frac{1}{2}$ states. A small mixing angle between them, $|\phi| < 6°$, is shown to be compatible with the experimental restriction on the width of $D_{s1}(2536)$, admitting the possible admixture of other component in the wave function (w.f.) $\lesssim 10\%$.

In our analysis the 4-component (Dirac) structure of the light-quark w.f. is crucially important. Specifically, the emission of a NG meson is accompanied by the γ_5 factor which permutes higher and lower components of the Dirac bispinors. For the $j = 1/2$, P-wave and the $j = 1/2$, S-wave states, it is exactly the case that this "permuted overlap" of the w.f. is maximal because the lower component of the first state is similar to the higher component of the second state and vice versa. We do not know other examples of such "fine-tuning." On the other hand, in the first approximation we neglect an interaction between two mesons in the continuum, like DK, etc.

In the present paper we concentrate on the P-wave B, B_s mesons and the effects of the channel coupling. While the $1P$ levels of the D, D_s mesons are now established with good accuracy [1,2,26], for the B, B_s mesons only relatively narrow 2^+, 1^+ states have recently been observed [27,28]. According to these data the splitting between the 2^+ and 1^+ levels is small, $\sim 20 - 10$ MeV, while the mass difference between $B_s(2^+)$ and $B(2^+)$ states is again $\sim$100 MeV, as for the $D_s(2^+)$ and $D(2^+)$ mesons.

The actual position of the $B(1P)$, $B_s(1P)$ levels is important for several reasons. First, since the dynamics of the $(q\bar{b})$ mesons is very similar to that of $q\bar{c}$, the observation of predicted large mass shifts of the $B_s(0^+, 1^{+'})$ levels would give a strong argument in favor of the decay channel mechanism suggested here and in [18]. It has been shown in [29] that the mass of $B_s(0^+)$ can change by 150 MeV in different chiral models. Second, experimental observation of all P-wave states for the B, B_s mesons could clarify many unclear features of spin-orbit and tensor interactions in mesons. Understanding of the DCC mass shifts could become an important step in constructing chiral theory of strong decays with emission of one or several NG particles.

The paper is organized as follows. In the next section we discuss the formalism from [18], extending it to the case of the B and B_s mesons, and also to the 1^+ states, and discuss the mixing between the 1^+ and $1^{+'}$ states. In Sec. III the masses of HL mesons, calculated in closed-channel approximation, are given. Section IV is devoted to the mechanism of chiral transitions, while in Sec. V our calculations of the mass shifts due to DCC are presented. The predictions of the $B(J^P)$, $B_s(J^P)$ masses and discussions of our results are given in Sec. VI, while Sec. VII contains the Conclusions. In Appendix A a connection between the lowest order of $\Delta L_{\rm FCM}$ and the effective Lagrangian is illustrated. In Appendix B the details of our calculations of the masses are given, while in Appendix C the connection between FS splittings and the mixing matrix of the 1^+ states is discussed.

II. MIXING OF THE 1^+ AND $1^{+'}$ STATES

It is well known that in the single-channel approximation, due to spin-orbit and tensor interactions, the P-wave multiplet of a HL meson is split into four levels with $J^P = 0^+, 1^+_L, 1^+_H, 2^+$ [30]. Here we use the notation H(L) for the higher (lower) 1^+ eigenstate of the mixing matrix because *a priori* one cannot say which of them mostly consists of the light-quark $j = 1/2$ contribution (see Appendix C). For a HL meson, strongly coupled to a nearby decay channel (DC), some member(s) of the P-wave multiplet can be shifted down while others cannot. Just such a situation takes place for the $D_s(1P)$ multiplet. The position of the levels with $j = \frac{3}{2}$, which remains unshifted, will be important in our analysis.

The scheme of classification, adapted to a HL meson, in the first approximation treats the heavy quark as a static one, and therefore the Dirac equation can be used to define the light-quark levels and wave functions [10]. Starting with the Dirac's P-wave levels, one has the states with $j = 1/2$ and $j = 3/2$. Since the light-quark momentum j and the quantum number $\varkappa$ are conserved,[1] they run along the following possible values:

[1]Here we use the standard notation $\varkappa = \mp|j + \frac{1}{2}|$ for

$$j = \begin{cases} l + \frac{1}{2}, \\ l - \frac{1}{2}. \end{cases}$$

$$
\begin{array}{cccc}
\multicolumn{4}{l}{\text{even } l} \\
J^P & j & l & \varkappa \\
0^- & \frac{1}{2} & 0 & -1 \\
1^- & \frac{1}{2} & 0 & -1 \\
1^- & \frac{3}{2} & 2 & +2
\end{array}
\qquad
\begin{array}{cccc}
\multicolumn{4}{l}{\text{odd } l} \\
J^P & j & l & \varkappa \\
0^+ & \frac{1}{2} & 1 & +1 \\
1^+ & \frac{1}{2} & 1 & +1 \\
1^+ & \frac{3}{2} & 1 & -2 \\
2^+ & \frac{3}{2} & 1 & -2 \\
2^+ & \frac{5}{2} & 3 & +3
\end{array}
\tag{2}
$$

The HL meson w.f. can be expressed in terms of the light-quark w.f.—the Dirac bispinors $\psi_{q,s}^{jlM}$:

$$
\begin{aligned}
\Psi_D(J^-_{1/2}, M_f) = {} & C^{J,M_f}_{1/2,M_f-(1/2);1/2,+(1/2)} \psi_q^{1/2,0,M_f-(1/2)} \otimes |\bar{c}\uparrow\rangle \\
& + C^{J,M_f}_{1/2,M_f+(1/2);1/2,-(1/2)} \\
& \times \psi_q^{1/2,0,M_f+(1/2)} \otimes |\bar{c}\downarrow\rangle,
\end{aligned}
\tag{3}
$$

$$
\begin{aligned}
\Psi_{D_s}(J^+_j, M_i) = {} & C^{J,M_i}_{j,M_i-(1/2);1/2,+(1/2)} \psi_s^{j,1,M_i-(1/2)} \otimes |\bar{c}\uparrow\rangle \\
& + C^{J,M_i}_{j,M_i+(1/2);1/2,-(1/2)} \psi_s^{j,1,M_i+(1/2)} \otimes |\bar{c}\downarrow\rangle,
\end{aligned}
\tag{4}
$$

where $C^{JM}_{j_1M_1;j_2M_2}$ are the corresponding Clebsch-Gordan coefficients.

Later in the w.f. we neglect possible (very small) mixing between the $D(1^-_{1/2})$, $D(1^-_{3/2})$ states and also between $D_s(2^+_{3/2})$, $D_s(2^+_{5/2})$ states. However, physical $D_s(1^+)$ states can be mixed via open channels and tensor interaction, while the 0^+ and 2^+ levels are obtained solely from $j = \frac{1}{2}$ and $j = \frac{3}{2}$, respectively.

The eigenstates, defining the higher 1^+_H and lower 1^+_L levels, can be parametrized by introducing the mixing angle ϕ:

$$|1^+_H\rangle = \cos\phi|j = \tfrac{1}{2}\rangle + \sin\phi|j = \tfrac{3}{2}\rangle \tag{5}$$

and

$$|1^+_L\rangle = -\sin\phi|j = \tfrac{1}{2}\rangle + \cos\phi|j = \tfrac{3}{2}\rangle, \tag{6}$$

where the mixing angle is defined by the unitary mixing matrix $\hat{O}_{\text{mix}}$, given in Appendix C. In the heavy-quark (HQ) limit the states with $j = \frac{3}{2}$ and $j = \frac{1}{2}$ are not mixed, but for finite m_Q they can be mixed even in the closed-channel approximation [10,30]. Here we follow the approach developed in [30]. Then if one neglects the terms proportional to m_Q^{-2} (m_Q is a HQ mass), the mixing matrix $\hat{O}_{\text{mix}}$ and ϕ are defined by only the ratio a/t, where a is the spin orbit and t is the tensor splitting (their definition is given below and in Appendix C). This fact simplifies our analysis because we do not need to know details of spin-orbit interaction, which at present are not fully understood.

The states 1^+_L and 1^+_H in (5) and (6) can also be expressed through the mixing angle θ in the **LS** basis, where they represent the decomposition of the $^3P_1$ and $^1P_1$ states:

$$
\begin{aligned}
|1^+_H &= \cos\theta|^3P_1\rangle - \sin\theta|^1P_1\rangle, \\
|1^+_L &= \sin\theta|^3P_1\rangle + \cos\theta|^1P_1\rangle.
\end{aligned}
\tag{7}
$$

Then, using the relations between the $^3P_1$, $^1P_1$ states and the eigenstates $|j = \frac{3}{2}\rangle$, $|j = \frac{1}{2}\rangle$ [30],

$$
\begin{aligned}
|^3P_1\rangle &= \frac{1}{\sqrt{3}}\left|j = \frac{3}{2}\right\rangle + \sqrt{\frac{2}{3}}\left|j = \frac{1}{2}\right\rangle, \\
|^1P_1\rangle &= \sqrt{\frac{2}{3}}\left|j = \frac{3}{2}\right\rangle - \frac{1}{\sqrt{3}}\left|j = \frac{1}{2}\right\rangle,
\end{aligned}
\tag{8}
$$

the following relation can be established between angles ϕ and θ:

$$\phi = -\theta + 35.264°. \tag{9}$$

From (9) it follows that

(1) If 1^+_H is a pure $|j = \frac{1}{2}\rangle$ state ($\phi = 0°$), then in the **LS** basis this state is the admixture of the $^3P_1$ and $^1P_1$ states with $\theta = 35.264°$.

(2) If 1^+_H is a pure $|j = \frac{3}{2}\rangle$ state ($\phi = 90°$), then in the **LS** basis the mixing angle $\theta = -54.736°$.

(3) The special case with $\phi = -9.74°$ corresponds to "equal" mixing between the $^3P_1$ and $^1P_1$ states with the angle $\theta = -45°$.

Later we will show that just the 1^+_L level with small $|\phi| \lesssim 6°$ ($29° \lesssim \theta \lesssim 41°$), being an almost pure $j = \frac{3}{2}$ state, has no DC (hadronic) mass shift. In the opposite case, when 1^+_H is mostly a $j = \frac{3}{2}$ state, it is convenient to redefine in Eqs. (5) and (6) the mixing angle as $\gamma = 90° - \phi$, performing a similar analysis.

Our result (9) is in full agreement with the prediction in [31], where large mass shifts down $\sim$100 MeV for $D_s(1^{+'})$, $B_s(1^{+'})$ due to strong coupled-channel effects are obtained taking the mixing angle $\theta \simeq 35°$ (in our notations).

The dependence of the mixing angle ϕ on the ratio a/t is illustrated by the numbers in Table I. In the single-channel approximation SO and tensor splittings a, t of a P-wave multiplet are the universal numbers which are expressed via the experimental masses $M_J(1P)$: $M_0 \equiv M(0^+)$, $M_2 \equiv M(2^+)$, $M_1^H = M(1^+_H)$, $M_1^L = M(1^+_L)$:

TABLE I. The dependence of the mixing angle ϕ and the mass difference $\Delta_{3/2} = M(2^+) - M_1(j = \frac{3}{2})$ on the ratio a/t for OGE plus linear potential.

$\frac{a}{t}$	0.50	0.67	0.945[a]	1.0	1.1	1.3
ϕ	9.7°	14.7°	45°	54.7°	67.3°	78.1°
$P^L_{3/2} = \cos^2\phi$	0.971	0.935	0.50	0.33	0.15	0.04
$P^H_{3/2} = \sin^2\phi$	0.028	0.064	0.50	0.67	0.85	0.96
$\Delta_{3/2}/t$	1.11	1.13	1.30 0.83	0.90	0.97	1.02

[a]For $\phi = 45°$, i.e. for $P^L_{3/2} = P^H_{3/2} = 1/2$, there are two solutions for $\Delta_{3/2}$.

$$a(nP) = \frac{1}{48}\{25M_2 - 9(M_1^H + M_1^L) - 7M_0\},$$
$$t(nP) = \frac{5}{8}\{M_1^H + M_1^L - M_2 - M_0\}, \tag{10}$$
$$M_{\rm cog} = \frac{1}{12}\{M_0 + 3(M_1^H + M_1^L) + 5M_2\},$$

where $M_{\rm cog}$ is the multiplet center of gravity.

It is of interest to notice that the masses M_2 and M_0 are expressed via the splittings a, t, as well as in heavy quarkonia:

$$M(2^+) - M_{\rm cog} = a - 0.1t,$$
$$M(0^+) - M_{\rm cog} = -2a - t, \tag{11}$$
$$M(2^+) - M(0^+) = 3a - 0.9t,$$

where the numbers, preceding a, t, are the spin-averaged matrix elements (m.e.'s) which are calculated in [30]. The weight with which the eigenstates $j = \frac{3}{2}$ enter the level $1_H^+(1_L^+)$ is denoted here as $P_{3/2}^H = \sin^2\phi$ ($P_{3/2}^L = \cos^2\phi$). It is also convenient to introduce the mass difference $\Delta_{3/2} = M_2 - \tilde{M}_1(j = \frac{3}{2})$ between two narrow states: $M(2^+)$ and the mass $\tilde{M}_1$ of that 1^+ level for which $P_{3/2}$ is larger than $P_{1/2}$.

We expect that the 2^+ and $1^+(j = \frac{3}{2})$ levels are not affected by the DCC; therefore their mass difference $\Delta_{3/2}$ can be extracted from experimental data [26–28], having small experimental error [while from (10) $M_{\rm cog}$ has large error]:

$$\Delta_{3/2}(D) = M_2(2460) - M_1(2422) = 38.8 \pm 2.9 \text{ MeV},$$
$$\Delta_{3/2}(D_s) = M_2(2573) - M_1(2535) = 38.1 \pm 2.5 \text{ MeV},$$
$$\Delta_{3/2}(B) = \begin{cases} 26.2 \pm 4.0 \text{ MeV } (A) & \text{(D0 data [27])}, \\ 14.6 \pm 4.0 \text{ MeV } (B) & \text{(CDF data [28])}, \end{cases}$$
$$\Delta_{3/2}(B_s) = 10.2 \pm 0.6 \text{ MeV} \qquad \text{(CDF data [28])}. \tag{12}$$

At this point it is important to stress that the mixing matrix $\hat{O}_{\rm mix}$ used here is derived for the one-gluon-exchange (OGE) vector plus linear scalar potential, neglecting higher order radiative corrections and also the terms proportional to m_Q^{-2} as in [30]; therefore the dependence of the parameters ϕ, $P_{3/2}^{\rm H(L)}$, and $\Delta_{3/2}$ on the ratio a/t, presented in Table I, is an approximation and should be considered as an illustration.

The remarkable feature of the ratio $t^{-1}\Delta_{3/2}$ is that it weakly changes for large variations of a/t, and therefore it can be used to fit the tensor splitting. For fixed a/t the accuracy of the calculated tensor splitting appears to be 8% and about 15% for arbitrary a/t:

$$t_{\rm exp} = \frac{\Delta_{3/2}(\exp)}{1.05 \pm 0.15}. \tag{13}$$

From (13) one obtains that

$$t_{\rm exp}(D) \cong t_{\rm exp}(D_s) = 36 \pm 6 \text{ MeV};$$
$$t_{\rm exp}(B) = \begin{cases} 20 \pm 4 \text{ MeV} & \text{(D0 data [27])}, \\ 14 \pm 3 \text{ MeV} & \text{(CDF data [28])}, \end{cases} \tag{14}$$
$$t_{\rm exp}(B_s) = 10 \pm 2 \text{ MeV}.$$

For our analysis of the FS, it is essential that tensor splitting is much simpler than SO splitting in which large cancellation between perturbative (P) and nonperturbative (NP) terms is possible. Also if one directly extracts $a(nP)$ from (10), then for the $D(1P)$ multiplet (the only one for which all members are known), the splitting $a_{\rm exp}(D) = 29 \pm 18$ MeV has large experimental error and makes the ratio a/t uncertain.

The structure of the mixing is important because it defines the order of levels, the mass shift of the $1^{+\prime}$ state, as well as the mass shift and the width of another 1^+ level. One of our goals here is to understand why, if the coupling to the nearby continuum channel is taken into account, the position of the 2^+ and 1^+ levels does not change (within 1–3 MeV) while 0^+, $1^{+\prime}$ levels acquire large DC shifts.

III. THE MASSES OF HEAVY-LIGHT MESONS

In the closed-channel approximation the masses of HL mesons, or initial positions of the levels (without channel coupling), can be calculated in different schemes, e.g. in the **LS** coupling [18], or as in the Dirac-type coupling [10]. In Tables II and III we give these unperturbed masses for the B and B_s mesons which are calculated with the use of the relativistic string Hamiltonian [6,24]. In this approach, due to negative string corrections, the P-wave masses of HL mesons appear to be smaller than the eigenvalue (e.v.)

TABLE II. The B meson masses (in MeV) (without decay channel coupling). Cases A, B refer to $a/t = 0.67$, 1.20.

	0^-	1^-	0^+	1_L^+	1_H^+	2^+
From [20] and this paper	5279	5325	A. 5695	5726 ($j = 3/2$)	5740 ($j = 1/2$)	5745
			B. 5655	5710 ($j = 1/2$)	5726 ($j = 3/2$)	5745
Experiment	5279.0 ± 0.5 [26]	5325.0 ± 0.6 [15]		5721 ± 5 [28] $5725.3^{+2.4}_{-3.2}$ [32]		5746 ± 4 [28] $5739.9^{+2.2}_{-2.4}$ [32]

TABLE III. The B_s meson masses (in MeV) (without decay channel coupling). Cases A, B refer to $a/t = 0.67$, 1.20.

J^P	0^-	1^-	0^+	1^+_L	1^+_H	2^+
This paper and from [20]	5362	5407	A. 5814	5830 ($j = \frac{3}{2}$)	5835 ($j = \frac{1}{2}$)	5840
			B. 5795	5821 ($j = \frac{1}{2}$)	5830 ($j = \frac{3}{2}$)	
Experiment	5367.7 ± 1.8 [26]	5411.7 ± 3.2 [32]		5829.4 ± 0.8 [28]		5839.1 ± 3.0 [28]

of the spinless Salpeter equation in [3] and in some other potential models (see Tables II, III, IV, and V).

In our calculations we prefer not to fix the SO splitting and present the masses $M(1P)$ for two characteristic values: $a/t = 0.67$ and 1.20. The value $a/t = 1.20$ has some common features with the heavy-quark (HQ) limit.

For HL mesons, calculated masses of the 2^+, 1^+ states with $j = 3/2$ agree with experiment by derivation, while the mass difference $M_2 - M_0$ for the B meson varies from the value 50 MeV for $a/t = 0.67$ up to 90 MeV for $a/t = 1.20$. From here, one can conclude that knowledge of the mass $M(B(0^+))$ with good accuracy is crucially important for the understanding of the FS dynamics and, in particular, of the applicability of the HQ limit.

The masses given in Tables II and III are calculated with the use of (14), taking the tensor splitting $t \cong 17.7$ MeV and $t \cong 9$ MeV for the B and B_s mesons, respectively. In Table IV they are compared with the predictions in other models (there the conventional notations 1^+ and $1^{+'}$ for mainly $j = \frac{3}{2}$ and $j = \frac{1}{2}$ states are used).

TABLE IV. Theoretical predictions for the $B(1P)$ and $B_s(1P)$ masses (in MeV) (without decay channel coupling).

Reference	[3]	[4]	[10]	[14]	This paper $a/t = 0.67$ ($a/t = 1.2$)	Experiment[a,b]
$M_B(0^+)$	5760	5738	5706	5700	5695 (5655)	abs
$M_B(1^{+'})$	5780	5757	5742	5750	5740 (5710)	abs
$M_B(1^+)$	5780	5719	5700	5774	5726 (5726)	5721 (5)[a] 5725 (3)[b]
$M_B(2^+)$	5800	5733	5714	5790	5745 (5745)	5745 (4)[a] 5745 (2)[b]
$M_{B_s}(0^+)$	5830	5841	5804	5710	5814 (5795)	abs
$M_{B_s}(1^{+'})$	5860	5859	5842	5770	5835 (5821)	abs
$M_{B_s}(1^+)$	5860	5831	5805	5870	5830 (5830)	5830 (1)[b]
$M_{B_s}(2^+)$	5888	5844	5820	5893	5840 (5840)	5839 (1)[b]

[a]Experimental data of the D0 Collaboration [27].
[b]Experimental data from [28].

Comparison of the masses from Table IV shows that in different papers the masses $M(B)$, $M(B_s)$ agree within ± 50 MeV; however, the order of the levels inside the $1P$ multiplet appears to be different. In particular, in [4,10] the 2^+ level has smaller mass than the $1^{+'}$, while in our calculations the 2^+ state always has maximal mass. It means that FS parameters a, t and their ratio, as well as the mixing angle ϕ, can essentially differ in different papers. Meanwhile, the existing experimental limit on the width of $D_{s1}(2535)$ puts strong restrictions on the admissible value of the mixing angle ϕ (see next section).

Finally, in Table V we also give unperturbed masses of the $D(1P)$ and $D_s(1P)$ mesons, taking again $a/t = 0.67$ and $a/t = 1.20$. Then from (11) for the given a/t the splittings $t_{\rm exp} = 33.5$ and 38 MeV, respectively, are obtained. From Table V one can see that in the case with $a/t = 0.67$, a better agreement with experiment is obtained for all $D(1P)$ mesons, even in the closed-channel approximation. For $a/t = 1.20$ the 0^+ state lies 75 MeV lower than in the former case, and the mass $M(1^{+'}) = 2390$ MeV is also 50 MeV lower than the central value $M_{\rm exp}(1^{+'}) = 2427(52)$ MeV in experiment. [The width of this meson (~ 380 MeV) is so large that the discrepancy $\sim$50 MeV seems to be inessential.] As a whole, we estimate the uncertainties in the values of initial (unperturbed) masses of $D_s(0^+)$ and $D_s(1^{+'})$ as ± 30 MeV and ± 15 MeV, and also ± 15 MeV for the $B_s(1P)$ mesons.

These theoretical uncertainties occur because, at present, the details of spin-orbit interaction are not fully understood, in particular, the role of one-loop (or even higher) corrections in P potentials (which can give $\sim$30% corrections even in heavy quarkonia [33]) and also the possible suppression of the NP spin-orbit potential, recently observed on the lattice [34].

Now we shortly discuss some features of the FS interaction in the HQ limit. To this end we take a, t in the simplest form when the vector interaction is defined by the OGE potential and the scalar part is given by the linear confining potential. Then

$$t(nP) = \frac{T}{\omega_1 \omega_2}; \qquad T(nP) = \frac{4}{3} \alpha_{\rm FS} \langle r^{-3} \rangle_{nP}, \tag{15}$$

$$a(nP) = \frac{1}{4\omega_1^2} A + t(nP), \tag{16}$$

TABLE V. The masses of the $D(1P)$ and $D_s(1P)$ mesons (in MeV) (without decay channel coupling). Cases A, B refer to $a/t = 0.67$, 1.2.

	0^+	1^+_L	1^+_H	2^+
D	A. 2365	2423	2450	2462
	B. 2290	2390	2425	2461
Experiment [26]	2350 ± 50	2422 ± 1.3	2427 ± 51	2459 ± 4
D_s	A. 2475	2537	2568	2575
	B. 2405	2505	2537	2575
Experiment [26]	2317.3 ± 0.6	2535.4 ± 0.8	2459 ± 1	2573.5 ± 1.7

with

$$A(nP) = \frac{4}{3}\alpha_{\mathrm{FS}}\langle r^{-3}\rangle_{nP} - \sigma\langle r^{-1}\rangle_{nP}. \tag{17}$$

In realistic calculations, even with rather large $\alpha_{\mathrm{FS}} \leq 0.5$, $A(nP)$ appears to be a negative (or very small) value and the presence of the second term $t(nP)$ in the SO splitting (16) is very important. In the HQ limit, $t \to 0$, $a_{\mathrm{HQL}} \to \frac{1}{4\omega_1^2}A$; therefore negative A gives rise to inverse order of the levels, i.e. $M(0^+) > M(2^+)$. Up to now there have been no such examples in the meson sector for low-lying states. However, one cannot exclude that such an order can occur for the $B(1P)$ mesons and their higher excitations. The case with $A > 0$, $a/t > 1$ can be realized only if the coupling α_{FS} is very large, and in this case (see Tables II, III, IV, and V) the mass difference, $M(2^+) - M(0^+)$, turns out to be essentially larger than in the case with $a/t \lesssim 0.7$.

For comparison we give a/t in heavy quarkonia when their values are close or equal to unity:

$$\begin{aligned} a/t &= 1.04 \pm 0.08 \quad \text{for } \chi_b(1P), \\ a/t &= (1.02 \pm 0.14) \quad \text{for } \chi_b(2P), \\ a/t &= (0.86 \pm 0.02) \quad \text{for } \chi_c(1P). \end{aligned} \tag{18}$$

IV. CHIRAL TRANSITIONS

To obtain the mass shift due to the DCC effect, we use here the chiral Lagrangian (1), which includes both effects of confinement (embodied in the string tension) and chiral symmetry breaking (CSB) (in Euclidean notations):

$$L_{\mathrm{FCM}} = i\int d^4x\psi^+(\hat\partial + m + \hat M)\psi \tag{19}$$

with the mass operator $\hat M$ given as a product of the scalar function $W(r)$ and the $SU(3)$ flavor octet,

$$\hat M = W(r)\exp\left(i\gamma_5\frac{\varphi_a\lambda_a}{f_\pi}\right), \tag{20}$$

where

$$\varphi_a\lambda_a = \sqrt{2}\begin{pmatrix} \frac{\pi^0}{\sqrt2} + \frac{\eta^0}{\sqrt6} & \pi^+ & K^+ \\ \pi^- & \frac{\eta^0}{\sqrt6} - \frac{\pi^0}{\sqrt2} & K^0 \\ K^- & \bar K^0 & -\frac{2\eta^0}{\sqrt6} \end{pmatrix}. \tag{21}$$

Taking the meson emission to the lowest order, one obtains the quark-pion Lagrangian in the form

$$\Delta L_{\mathrm{FCM}} = -\int \psi_i^+(x)\sigma|\mathbf{x}|\gamma_5\frac{\varphi_a\lambda_a}{f\pi}\psi_k(x)d^4x. \tag{22}$$

Writing Eq. (22) as $\Delta L_{\mathrm{FCM}} = -\int V_{if}dt$, one obtains the operator matrix element for the transition from the light-quark state i (i.e. the initial state i of a HL meson) to the continuum state f with the emission of a NG meson $(\varphi_a\lambda_a)$. Thus we are now able to write the coupled-channel equations, connecting any state of a HL meson to a decay channel which contains another HL meson plus a NG meson.

In the case when interaction in each channel and also in the transition operator is time independent, one can write the following system of equations (see [35] for a review):

$$[(H_i - E)\delta_{il} + V_{il}]G_{lf} = 1. \tag{23}$$

Such a two-channel system of equations can be reduced to one equation with an additional DCC potential, or the Feshbach potential [36],

$$(H_1 - E)G_{11} - V_{12}\frac{1}{H_2 - E}V_{21}G_{11} = 1. \tag{24}$$

Considering a complete set of the states $|f\rangle$ in decay channel 2 and a set of unperturbed states $|i\rangle$ in channel 1, one arrives at the nonlinear equation for the shifted mass E,

$$E = E_1^{(i)} - \sum_f\langle i|V_{12}|f\rangle\frac{1}{E_2^{(f)} - E}\langle f|V_{21}|i\rangle. \tag{25}$$

Here the unperturbed values of $E_1^{(i)}$ are assumed to be known (see Tables II, III, and V), while the interaction U_{if} is defined in (22). A solution of the nonlinear equation (25) yields (in general, a complex number $E = \bar E - \frac{i\Gamma}{2}$) one or more roots on all Riemann sheets of the complex mass plane.

V. CALCULATION OF THE DCC SHIFTS

To calculate explicitly the mass shifts, we will use Eq. (25) in the following form:

$$m[i] = m^{(0)}[i] - \sum_f \frac{|\langle i|\hat{V}|f\rangle|^2}{E_f - m[i]}, \tag{26}$$

where $m^{(0)}[i]$ is the initial mass, $m[i]$ is the final one, $E_f = \omega_D + \omega_K$ is the energy of the final state, and the operator $\hat{V}$ provides the transitions between the channels [see the comment after Eq. (22)].

In our approximation we do not take into account the final state interaction in the DK system, and we neglect the D-meson motion, so the w.f. of the i, f states are

$$|f\rangle = \Psi_K(\mathbf{p}) \otimes \Psi_D(M_f), \qquad |i\rangle = \Psi_{D_s}(M_i), \tag{27}$$

where

$$\Psi_K(\mathbf{p}) = \frac{e^{i\mathbf{pr}}}{\sqrt{2\omega_K(\mathbf{p})}} \tag{28}$$

is the plane wave describing the K meson and $\Psi_D(M_f)$, $\Psi_{D_s}(M_i)$ are the HL meson w.f. at rest with the spin projections M_f, M_i, respectively.

We introduce the following notations:

$$\omega_K(\mathbf{p}) = \sqrt{\mathbf{p}^2 + m_K^2}, \qquad \omega_D(\mathbf{p}) = \sqrt{\mathbf{p}^2 + m_D^2}, \tag{29}$$

so that in the final state the total energy is $E_f = \omega_D + \omega_K$, while

$$T_f = E_f - m_D - m_K \tag{30}$$

is the kinetic energy. Also it is convenient to define other masses with respect to the nearby threshold: $m_{\text{thr}} = m_K + m_D$,

$$E_0 = m^{(0)}[D_s] - m_D - m_K, \qquad \delta m = m[D_s] - m^{(0)}[D_s], \tag{31}$$

$$\Delta = E_0 + \delta m = m[D_s] - m_D - m_K, \tag{32}$$

where Δ determines the deviation of the D_s meson mass from the threshold. In what follows we consider unperturbed masses $m_0(J^P)$ of the $(Q\bar{q})$ levels as an input; actually our results do not change if we slightly vary their position (thus the analysis is quite model independent).

Using these notations, Eq. (25) can be rewritten as

$$E_0 - \Delta = \mathcal{F}(\Delta), \tag{33}$$

where

$$\mathcal{F}(\Delta) \stackrel{\text{def}}{=} \int \frac{d^3\mathbf{p}}{(2\pi)^3} \sum_{M_f} \frac{|\langle M_i|\hat{V}|\mathbf{p}, M_f\rangle|^2}{T_f(\mathbf{p}) - \Delta} \tag{34}$$

and

$$\langle M_i|\hat{V}|\mathbf{p}, M_f\rangle = -\int \Psi^\dagger_{D_s}(M_i)\sigma|\mathbf{r}|\gamma_5 \frac{\sqrt{2}}{f_K}\Psi_D(M_f) \times \frac{e^{i\mathbf{pr}}}{\sqrt{2\omega_K(\mathbf{p})}} d^3\mathbf{r}. \tag{35}$$

The function $\mathcal{F}(\Delta)$ for negative Δ diminishes monotonously so there exists a final (critical) point,

$$E_0^{\text{crit}} = \mathcal{F}(-0). \tag{36}$$

Thus, while solving Eq. (33), one has two possible situations: $E_0 < E_0^{\text{crit}}$ and $E_0 > E_0^{\text{crit}}$.

In the first case Eq. (33) has a negative real root $\Delta < 0$ (see Fig. 1) and the resulting mass of the D_s meson appears to be under the threshold. In the second case Eq. (33) has a complex root $\Delta = \Delta' + i\Delta''$ with a positive real part $\Delta' > 0$ (see Fig. 2) and a negative imaginary part $\Delta'' < 0$. To find the latter solutions one should make an analytic continuation of the solution(s) from the upper half-plane of Δ under the cut, which starts at the threshold, to the lower half-plane (second sheet). This solution can also be obtained by deforming the integration contour in $T_f(p)$. In actual calculations we take the infinitesimal imaginary part Δ'', proving that Δ does not change much for finite Δ'' (a similar procedure has been used in [18]). Finally, the resulting mass of the D_s meson proves to be in the complex plane at the position $\Delta' - i|\Delta''|$, i.e. the meson has the finite width $\Gamma = 2\Delta''$.

To proceed further we should insert the explicit meson w.f. into the matrix element (35). As discussed above, in a HL meson we consider a light quark q moving in the static field of a heavy antiquark $\bar{Q}$, and therefore its w.f. can be taken as the Dirac bispinor:

$$\psi_q^{jlM} = \begin{pmatrix} g(r)\Omega_{jlM} \\ (-1)^{(1+l-l')/2} f(r)\Omega_{jl'M} \end{pmatrix}, \tag{37}$$

$$\int_0^\infty (f^2 + g^2) r^2 dr = 1,$$

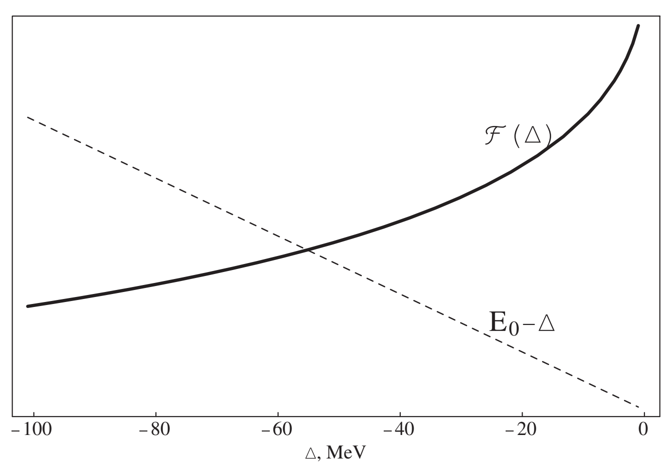

FIG. 1. Equation (33) for the case $E_0 < E_0^{\text{crit}}$.

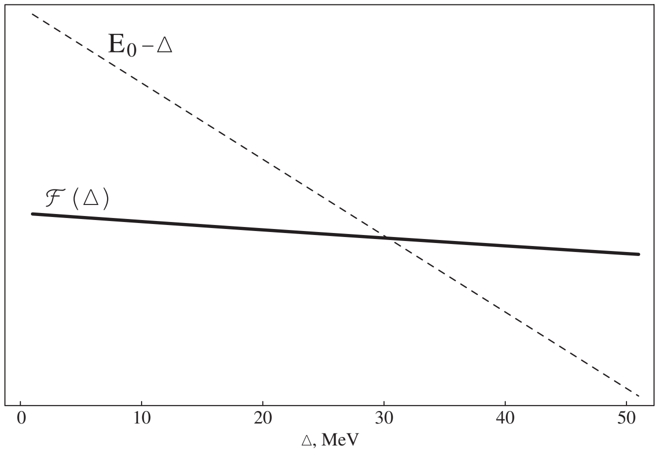

FIG. 2. Equation (33) for the case $E_0 > E_0^{\rm crit}$.

where the functions $g(r)$ and $f(r)$ are the solutions of the Dirac equation:

$$g' + \frac{1+\varkappa}{r}g - (E_q + m_q + U - V_C)f = 0,$$
$$f' + \frac{1-\varkappa}{r}f + (E_q - m_q - U - V_C)g = 0. \tag{38}$$

Here the interaction between the quark and the antiquark is described by a sum of the linear scalar potential and the vector Coulomb potential with $\alpha_s = \text{const}$:

$$U = \sigma r, \qquad V_C = -\frac{\beta}{r}, \qquad \beta = \frac{4}{3}\alpha_s. \tag{39}$$

Introducing new dimensionless variables

$$x = r\sqrt{\sigma}, \qquad \varepsilon_q = E_q/\sqrt{\sigma}, \qquad \mu_q = m_q/\sqrt{\sigma}, \tag{40}$$

and new dimensionless functions

$$g = \sigma^{3/4}\frac{G(x)}{x}, \qquad f = \sigma^{3/4}\frac{F(x)}{x},$$
$$\int_0^\infty (F^2 + G^2)dx = 1, \tag{41}$$

we come to the following system of equations:

$$G' + \frac{\varkappa}{x}G - \left(\varepsilon_q + \mu_q + x + \frac{\beta}{x}\right)F = 0,$$
$$F' - \frac{\varkappa}{x}F + \left(\varepsilon_q - \mu_q - x + \frac{\beta}{x}\right)G = 0. \tag{42}$$

This system has been solved numerically.

Using the parameters from the papers [37],

$$\sigma = 0.18\ \text{GeV}^2, \qquad \alpha_s = 0.39,$$
$$m_s = 210\ \text{MeV}, \qquad m_q = 4\ \text{MeV}, \tag{43}$$

we obtain the following Dirac eigenvalues ε:

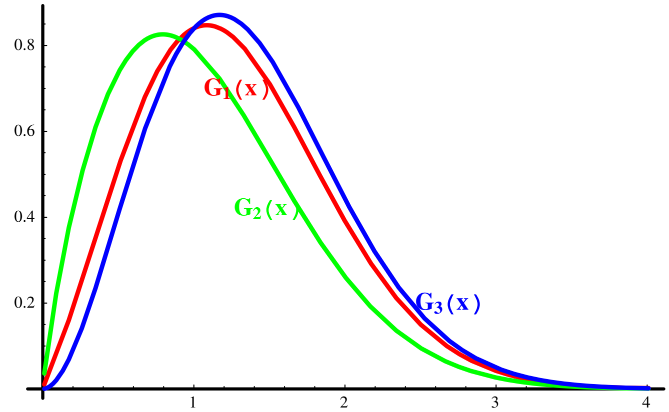

FIG. 3 (color online). $G_{1,2,3}(x)$ functions.

$$\begin{array}{ccc} \varkappa & \bar{Q}q,\ \mu_q = 0.01 & \bar{Q}s,\ \mu_s = 0.5 \\ -1 & 1.0026 & 1.289\,44 \\ +1 & 1.7829 & 2.086\,07 \\ -2 & 1.7545 & 2.084\,75 \end{array} \tag{44}$$

and the corresponding eigenfunctions G, F are given in Figs. 3 and 4.

Later we use the simplified notations for the quark bispinors:

$$\psi_1(M_1) \stackrel{\rm def}{=} \psi_s^{1/2,1,M_1}, \qquad \psi_2(M_2) \stackrel{\rm def}{=} \psi_q^{1/2,0,M_2},$$
$$\psi_3(M_3) \stackrel{\rm def}{=} \psi_s^{3/2,1,M_3}. \tag{45}$$

Now, using explicit expressions for the spherical spinors,

$$\Omega_{l+1/2,l,M} = \begin{bmatrix} \sqrt{\frac{j+M}{2j}}Y_{l,M-1/2} \\ \sqrt{\frac{j-M}{2j}}Y_{l,M+1/2} \end{bmatrix},$$
$$\Omega_{l-1/2,l,M} = \begin{bmatrix} -\sqrt{\frac{j-M+1}{2j+2}}Y_{l,M-1/2} \\ \sqrt{\frac{j+M+1}{2j+2}}Y_{l,M+1/2} \end{bmatrix}, \tag{46}$$

and the expansion

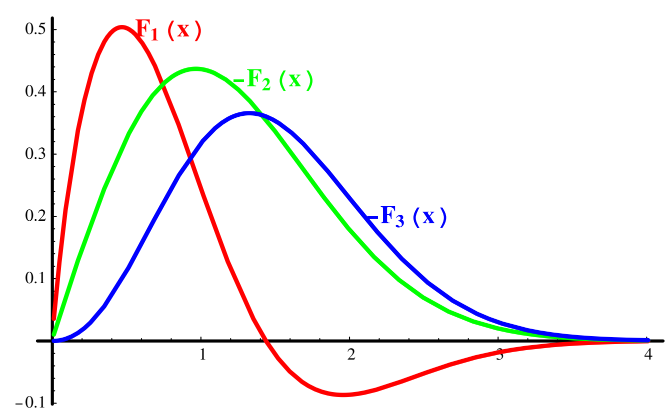

FIG. 4 (color online). $F_{1,2,3}(x)$ functions.

$$e^{i\mathbf{pr}} = 4\pi\sum_{l,M} i^l j_l(pr) Y^*_{l,M}\left(\frac{\mathbf{p}}{p}\right) Y_{l,M}\left(\frac{\mathbf{r}}{r}\right), \tag{47}$$

after cumbersome transformations (which are omitted in the text), we obtain the transition matrix elements:

$$\begin{aligned} \| \mathcal{V}_{12} \|_{M_1,M_2} &= -\int \psi_1^\dagger(M_1)\sigma|\mathbf{r}|\gamma_5 \frac{\sqrt{2}}{f_K}\psi_2(M_2)\frac{e^{i\mathbf{pr}}}{\sqrt{2\omega_K(\mathbf{p})}} d^3\mathbf{r} \\ &= \frac{\sqrt{\sigma}}{f_K\sqrt{\omega_K(p)}}\Phi_0\left(\frac{p}{\sqrt{\sigma}}\right)\sqrt{4\pi}Y^*_{0,M_1-M_2}\left(\frac{\mathbf{p}}{p}\right), \end{aligned} \tag{48}$$

$$\begin{aligned} \| \mathcal{V}_{32} \|_{M_3,M_2} &= -\int \psi_3^\dagger(M_3)\sigma|\mathbf{r}|\gamma_5 \frac{\sqrt{2}}{f_K}\psi_2(M_2)\frac{e^{i\mathbf{pr}}}{\sqrt{2\omega_K(\mathbf{p})}} d^3\mathbf{r} \\ &= -\frac{\sqrt{\sigma}}{f_K\sqrt{\omega_K(p)}}\Phi_2\left(\frac{p}{\sqrt{\sigma}}\right)\sqrt{\frac{4\pi}{5}}Y^*_{2,M_3-M_2}\left(\frac{\mathbf{p}}{p}\right) \\ &\quad\times\begin{bmatrix} -1 & +2 \\ -\sqrt{2} & +\sqrt{3} \\ -\sqrt{3} & +\sqrt{2} \\ -2 & +1 \end{bmatrix}, \end{aligned} \tag{49}$$

where

$$\begin{aligned} \Phi_0(q) &= \int_0^\infty j_0(qx)xdx[G_1(x)F_2(x) - F_1(x)G_2(x)], \\ \Phi_2(q) &= \int_0^\infty j_2(qx)xdx[G_3(x)F_2(x) - F_3(x)G_2(x)]. \end{aligned} \tag{50}$$

Notice that because of different signs of the $F_1(x)$ and $F_{2,3}(x)$ functions (while the $G_{1,2,3}$ functions are all positive) on almost all real axes, the integral Φ_2 appears to be strongly suppressed in comparison with the integral Φ_0. This fact is confirmed by numerical simulations (see Fig. 5).

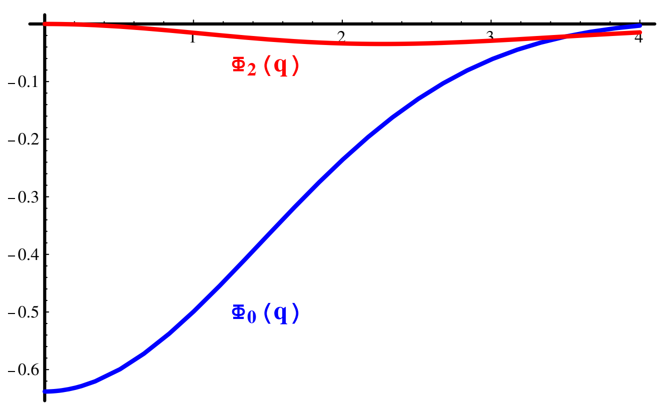

FIG. 5 (color online). $\Phi_{0,2}(q)$ functions.

Finally, introducing universal functions

$$\begin{aligned} \tilde{\mathcal{F}}_{0,2}(\Delta) &= \frac{\sigma}{2\pi^2 f_K^2}\int_0^\infty \frac{p(T_f)\omega_D(T_f)dT_f}{T_f + m_D + m_K}\cdot\frac{\Phi^2_{0,2}(\frac{p(T_f)}{\sqrt{\sigma}})}{T_f - \Delta}, \\ \tilde{\Gamma}_{0,2}(T_f) &= \frac{\sigma}{\pi f_K^2}\cdot\frac{p(T_f)\omega_D(T_f)}{T_f + m_D + m_K}\cdot\Phi^2_{0,2}\left(\frac{p(T_f)}{\sqrt{\sigma}}\right), \end{aligned} \tag{51}$$

we come to the following equations to determine meson masses and widths:

$$\begin{array}{ll} D_s(0^+) & E_0[0^+] - \Delta = \tilde{\mathcal{F}}_0(\Delta), \\ D_s(1_L^+) & E_0[1_L^+] - \Delta = \cos^2\phi\cdot\tilde{\mathcal{F}}_0(\Delta) + \sin^2\phi\cdot\tilde{\mathcal{F}}_2(\Delta), \\ D_s(1_H^+) & E_0[1_H^-] - \Delta' = \sin^2\phi\cdot\tilde{\mathcal{F}}_0(\Delta') + \cos^2\phi\cdot\tilde{\mathcal{F}}_2(\Delta'), \\ & \Gamma[1_H^+] = \sin^2\phi\cdot\tilde{\Gamma}_0(\Delta') + \cos^2\phi\cdot\tilde{\Gamma}_2(\Delta'), \\ D_s(2^+_{3/2}) & E_0[2^+_{3/2}] - \Delta' = \frac{3}{5}\cdot\tilde{\mathcal{F}}_2(\Delta'), \\ & \Gamma[2^+_{3/2}] = \frac{3}{5}\cdot\tilde{\Gamma}_2(\Delta'). \end{array} \tag{52}$$

VI. RESULTS AND DISCUSSION

In this section, using the expressions (52) to define the D_s- and B_s-meson mass shifts, we present and discuss our results. We will take into account the following pairs of mesons in coupled channels [i refers to the first (initial) channel, while f refers to the second (decay) one]:

$$\begin{array}{llll} i & D_s(0^+) & D_s(1^+) & D_s(2^+) \\ f & D(0^-) + K(0^-) & D^*(1^-) + K(0^-) & D^*(1^-) + K(0^-) \\ i & B_s(0^+) & B_s(1^+) & B_s(2^+) \\ f & B(0^-) + K(0^-) & B^*(1^-) + K(0^-) & B^*(1^-) + K(0^-) \end{array} \tag{53}$$

In our calculations we use the following meson masses and thresholds (in MeV):

$$\begin{aligned} m_{D^+} &= 1869, & m_{D^+} + m_{K^-} &= 2363, \\ m_{D^{*+}} &= 2010, & m_{D^{*+}} + m_{K^-} &= 2504, \\ m_{B^+} &= 5279, & m_{B^+} + m_{K^-} &= 5772, \\ m_{B^*} &= 5325, & m_{B^*} + m_{K^-} &= 5819. \end{aligned} \tag{54}$$

The results of our calculations are presented in Tables VI, VII, and VIII. *A priori* one cannot say whether the $|j = \frac{1}{2}\rangle$ and $|j = \frac{3}{2}\rangle$ states are mixed or not. For the case of no mixing, the width $\Gamma(D_{s1}(2536)) = 0.3$ MeV was calculated in [38], while the experimental limit is $\Gamma <$

TABLE VI. $D_s(0^+)$-meson mass shift due to the DK decay channel, and $B_s(0^+)$-meson mass shift due to the BK decay channel (all in MeV).

State	$m^{(0)}$	$m^{(\mathrm{theor})}$	$m^{(\mathrm{exp})}$	δm
$D_s(0^+)$	2475 (30)	2330 (20)	2317	−145
$B_s(0^+)$	5814 (15)	5709 (15)	not seen	−105

TABLE VII. The $D_s(1^+)$, $D_s(2^+)$-meson mass shifts and widths due to the D^*K decay channel for the mixing angle 4° (all in MeV).

State	$m^{(0)}$	$m^{(\mathrm{theor})}$	$m^{(\mathrm{exp})}$	$\Gamma^{(\mathrm{theor})}_{(D^*K)}$	$\Gamma^{(\mathrm{exp})}_{(D^*K)}$	δm
$D_s(1^+_H)$	2568 (15)	2458 (15)	2460	×	×	−110
$D_s(1^+_L)$	2537	2535 (15)	2535 (1)	1.1	<1.3	−2
$D_s(2^+_{3/2})$	2575	2573	2573 (2)	0.03	not seen	−2

TABLE VIII. The $B_s(1^+)$, $B_s(2^+)$-meson mass shifts and widths due to the B^*K decay channel for the mixing angle 4° (all in MeV).

State	$m^{(0)}$	$m^{(\mathrm{theor})}$	$m^{(\mathrm{exp})}$	$\Gamma^{(\mathrm{theor})}_{(B^*K)}$	$\Gamma^{(\mathrm{exp})}_{(B^*K)}$	δm
$B_s(1^+_H)$	5835 (15)	5727	not seen	×	×	−108
$B_s(1^+_L)$	5830 (fit)	5828	5829 (1)	0.8	<2.3	−2
$B_s(2^+_{3/2})$	5840 (fit)	5838	5839 (1)	$<10^{-3}$	not seen	−2

2.3 MeV [26] and recently in [39] the width $\Gamma = 1.0 \pm 0.17$ MeV has been measured. Therefore small mixing is not excluded, and here we take the mixing angle ϕ slightly deviated from $\phi = 0°$ (the no mixing case). Then we define those angles ϕ which are compatible with experimental data for the masses and widths of both 1^+ states. The mixing coefficients for the limiting angle $|\phi| = 5.7°$ are given in Table IX [this angle corresponds to the mixing between the $^3P_1$ and $^1P_1$ states with $\theta = 41°(29°)$ in the **LS** scheme].

TABLE IX. The mixing coefficients in Eq. (52) for the DCC shifts of the B_s, D_s mesons ($\phi = 5.7°$).

	1^+_H	1^+_L
$D_s(1P)$, $B_s(1P)$	$\cos^2\phi$ $(0.995)^2$	$\sin^2\phi$ $(0.100)^2$

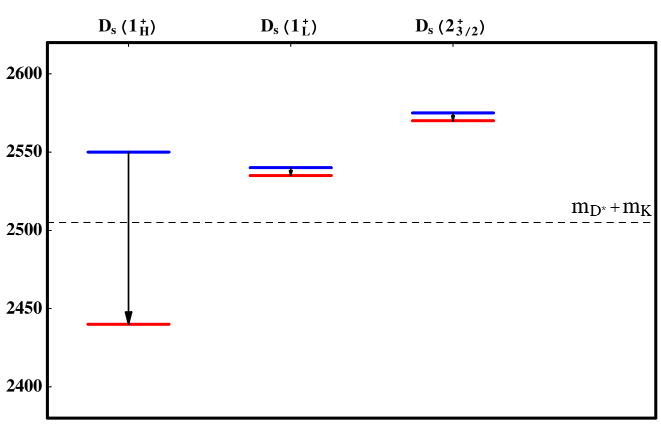

FIG. 6 (color online). Scheme of $D_s(1^+, 2^+)$ shifts due to chiral coupling.

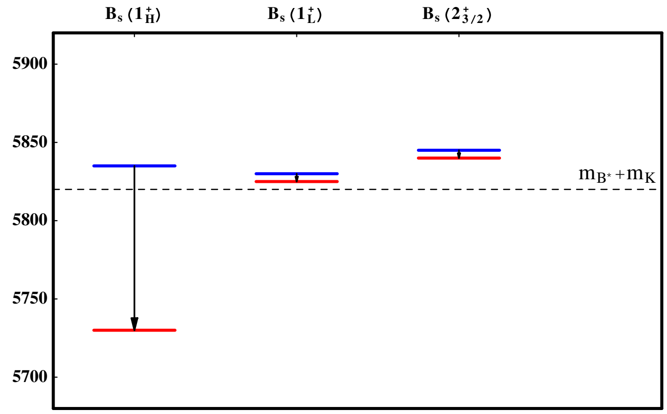

FIG. 7 (color online). Scheme of $B_s(1^+, 2^+)$ shifts due to chiral coupling.

The large value $\xi = (0.995)^2 = \cos^2\phi$ for the $1^+_H(j = 1/2)$ state provides a large mass shift (~ 100 MeV) of this level and, at the same time, does not produce the mass shift of the 1^+_L level, which is an almost pure $j = \frac{3}{2}$ state. For illustration we show the scheme of the 1^+, 2^+ shifts in Figs. 6 and 7. We would like to stress here that the mass shifts weakly differ for D_s and B_s, or weakly depend on the heavy-quark mass: this can be directly illustrated using in Eq. (52) the expansion via the inverse heavy-quark mass.

Thus we have obtained the shifted masses $M(B_s, 0^+) = 5710(15)$ MeV and $M(B_s, 1^{+'}) = 5730(15)$ MeV, which are in agreement with the predictions in [14] and of S. Narison [9], and $\sim$100 MeV lower than in [3,4,10]. The masses of the 2^+ and 1^+ states precisely agree with experiment because (13) is used to fit the tensor splitting.

The value of the tensor splittings, $t \cong 35$ MeV for the D and D_s mesons, corresponds to $\alpha_s(\mu_{\mathrm{FS}}) \sim 0.45$, if the OGE plus linear potential (C4) is used. Then for this coupling the ratio $a/t = 0.6$ and $\phi = 10°$ is obtained. This result should be considered as an estimate, because due to higher order radiative corrections in the SO potential, the angle ϕ and a/t can change. Notice also that in the mixing matrix (C13) the terms with β, proportional to m_Q^{-2}, can decrease the mixing angle for negative A, as in our example; therefore the exact value of a/t, corresponding to small $|\phi| < 6°$, cannot be defined with good accuracy.

VII. CONCLUSIONS

We have studied the mass shifts of the $D_s(0^+, 1^{+'})$ and $B_s(0^+, 1^{+'})$ mesons due to strong coupling to the decay channels DK, D^*K and BK, B^*K. To this end the chiral quark-pion Lagrangian without fitting parameters has been used.

We have shown that the emission of a NG meson, accompanied with the γ_5 factor, gives rise to maximal overlapping between the higher component with $j = \frac{1}{2}$ of the P-wave meson (D_s, B_s) bispinor w.f. and the lower component (also with $j = \frac{1}{2}$) of the S-wave HL meson w.f. in the S-wave decay channel considered. Because of this effect, while taking the w.f. of the $1P$ and $1S$ states with the use of the Dirac equation, large mass shifts of the 0^+, $1^{+'}$ states are obtained.

The widths of $D_{s1}(2536)$ and $B_{s1}(5830)$ are also calculated. To satisfy the experimental condition $\Gamma(D_{s1}(2536)) < 2.3$ MeV, the following limit on the mixing angle ϕ (between the $|j = \frac{3}{2}\rangle$ and $|j = \frac{1}{2}\rangle$ states) is obtained: $|\phi| \lesssim 6°$. These restrictions imply that the mixing angle θ between the $^3P_1$ and $^1P_1$ states in the **LS** basis lies in the range $29° \lesssim \theta \lesssim 41°$.

For our analysis it is essential that the value of the tensor splitting t can be extracted from the mass difference, $M(2^+) - M(1^+)$, which is not affected by the coupling to the decay channel. The value of the SO splitting still remains unfixed, because $(0^+, 1^{+'})$ levels of the D meson have large experimental errors, while $B(0^+)$, $B(1^{+'})$ have not yet been observed. Their observation would be very important for theory. Because of uncertainty in our choice of a, predicted masses of $1^{+'}$ and 0^+ mesons have theoretical errors within ~20 MeV. For the D_s, B_s mesons with $J^P = 0^+, 1^{+'}$, the predicted mass shifts due to DC coupling are

(i) $M(B_s(0^+)) = 5710(15)$ MeV, which is slightly higher than $M(B(0^+) = 5675(20)$ MeV,

(ii) $M(B_s(1^{+'})) = 5730(15)$ MeV, which is close to $M(B_1(1^{+'})) = 5725(20)$ MeV.

ACKNOWLEDGMENTS

The authors would like to acknowledge support from the President Grant No. 4961.2008.2 for scientific schools. One of the authors (M. A. T.) acknowledges partial support from the President Grant No. MK-2130.2008.2 and the RFBR for partial support via Grant No. 06-02-17120.

APPENDIX A: CONNECTION BETWEEN THE CHIRAL QUARK-PION LAGRANGIAN AND THE EFFECTIVE CHIRAL LAGRANGIAN

The interaction of pions with quarks was introduced and developed in [21,22]; see [17] for recent applications. The effective chiral Lagrangian ΔL_{eff} contains one new parameter, g_A^q,

$$L_{\pi q} = \frac{g_A^q}{2f_\pi}\bar{\Psi}\gamma_\mu\gamma_5\boldsymbol{\tau}\Psi\partial^\mu\phi_\pi, \tag{A1}$$

and has the form of a pseudovector coupling, known from phenomenological applications in the pion-nucleon systems. As was argued in [21], g_A^q at large N_c tends to unity.

In Eq. (17) we have used another form of the quark-pion interaction, derived directly from the QCD Lagrangian in [20] and not containing new parameters,

$$\Delta L_{\text{FCM}}^{(1)} = \int \bar{\psi}(x)\sigma|\mathbf{x}|\gamma_5\frac{\pi^a\lambda^a}{f_\pi}\psi(x)d^4x. \tag{A2}$$

In [20] the connection between (A1) and (A2) was established, and here we repeat the derivation for the convenience of the readers.

Consider the application of (A2) to the case of pionic transition between states $\psi_1(x)$ and $\psi_2(x)$ of the quark in the heavy-light meson. Dirac equations for $\psi_i(x)$ can be written as

$$(\boldsymbol{\alpha}\mathbf{p} + \beta(m + \sigma|\mathbf{x}|) + V_{\text{coul}})\psi_1 = \varepsilon_1\psi_1, \tag{A3}$$

$$\bar{\psi}_2(-\boldsymbol{\alpha}\mathbf{p} + \beta(m + \sigma|\mathbf{x}|) + V_{\text{coul}}) = \varepsilon_2\bar{\psi}_2. \tag{A4}$$

Expressing in (A3) and (A4) the term $\sigma|\mathbf{x}|\gamma_5$ via $\boldsymbol{\alpha}\mathbf{p}$, βm, etc., and summing two equations, one gets

$$\Delta L_{\text{FCM}}^{(1)} = \frac{1}{2f_\pi}\bar{\psi}_2(-2m\gamma_5\hat{\pi} + \beta\gamma_5(\varepsilon_2 - \varepsilon_1)\hat{\pi} + \gamma_5\beta\boldsymbol{\alpha}\mathbf{p}\hat{\pi})\psi_1. \tag{A5}$$

Since $\gamma_i = -i\beta\alpha_i$, and $(\varepsilon_2 - \varepsilon_1)\hat{\pi} = i\frac{\partial}{\partial t}\hat{\pi}(t)$, $\hat{\pi}(t) \sim e^{-i(\varepsilon_2-\varepsilon_1)t}$, one can rewrite the last two terms in (A5) as $\gamma_\mu\gamma_5\partial_\mu\hat{\pi}$, and finally one arrives at

$$\Delta L_{\text{FCM}}^{(1)} = \frac{1}{2f_\pi}\bar{\psi}_2(-2m\gamma_5\hat{\pi} + \gamma_\mu\gamma_5\partial_\mu\hat{\pi})\psi_1. \tag{A6}$$

Comparing (A1) and (A6), one can see that in the chiral limit, $m_q \to 0$, two expressions coincide. However, for nonzero m, e.g. for a strange quark having the mass $m_s \sim 0.2$ GeV at a low scale ~1 GeV [40], the first term in (A6) becomes essential. Moreover, our expression (A2) is only the first term in the expansion of the exponent (15) in powers of the pion field, and therefore this general Lagrangian can be used for decay channels with the production of two or several pions.

APPENDIX B: MASSES OF HEAVY-LIGHT MESONS

To calculate masses and different m.e.'s of a HL meson ($q\bar{b}$, $q\bar{c}$, or $\bar{q}b$), we use here the relativistic string Hamiltonian $\hat{H}_\omega$, derived in [24]. For this Hamiltonian the spin-averaged mass $M_{\text{cog}}(nL)$ is given by the simple formula

$$M_{\text{cog}}(nL) = M_0(nL) + \Delta_{\text{SE}} + \Delta_{\text{str}}, \tag{B1}$$

where M_0 is the e.v. of the spin-independent part H_0 of the Hamiltonian $\hat{H}_\omega$, which coincides with the well-known spinless Salpeter Hamiltonian (SSH):

$$H_0 = \sqrt{\mathbf{p}^2 + m_q^2} + \sqrt{\mathbf{p}^2 + m_b^2} + V_0(r), \tag{B2}$$

$$H_0\varphi_{nL}(r) = M_0\varphi_{nl}(r). \tag{B3}$$

Since the mass (B1) contains a negative (string) correction, for a given static potential in our approach, the levels with $L \neq 0$ lie lower than for the SSH. Also, the mass (B1) does not contain an overall fitting constant but takes into account the NP self-energy term $\Delta_{\rm SE}$ for a light quark (which is calculated explicitly in [41]).

The static potential

$$V_0(r) = \sigma r - \frac{4}{3}\frac{\alpha_B(r)}{r} \tag{B4}$$

is taken here from [25], with the vector coupling $\alpha_B(r)$ for $n_f = 3$. The solutions of (B3) define $M_0(nL)$ and, in particular, the average kinetic energy terms:

$$\omega_q(nL) = \langle\sqrt{\mathbf{p}^2 + m_q^2}\rangle_{nL}, \qquad \omega_Q(nL) = \langle\sqrt{\mathbf{p}^2 + m_Q^2}\rangle_{nL}, \tag{B5}$$

which appear to be the dynamical (constituent) masses of a light quark ω_q and a heavy quark ω_Q, correspondingly. Their values for the B and B_s mesons are given in Table X together with the reduced mass: $\omega_{\rm red} = \frac{\omega_q\omega_b}{\omega_q+\omega_b}$.

As seen from Table X the kinetic energy of a light (strange) quark $\omega_q(1P)$ is not small, and this fact is important for the fine-structure analysis.

In the mass formula (B1) the correction $\Delta_{\rm SE}$ comes from the NP self-energy contribution. It is equal to zero for the b quark, while for the c quark it is very small ($\lesssim 20$ MeV) as compared to the pole c-quark mass, and therefore can be neglected. For a light quark, $\Delta_{\rm SE}$ has been defined in [41]:

$$\Delta_{\rm SE}(nL) = \delta - \frac{1.5\sigma\eta_q}{\pi\omega_q}, \tag{B6}$$

in which a small correction, $\delta \sim 3 \div 6$ MeV (defined in [25]), is neglected. The factor $\eta_{u(d)} = 1.0$ for a light quark and $\eta_s = 0.65$ for an s quark with $m_s \cong 200$ MeV.

The string correction $\Delta_{\rm str}$ for the $1P$-wave $B(B_s)$ mesons is equal to $\Delta_{\rm str} \approx -27(-21)$ MeV [25]. This negative contribution to $M_{\rm cog}$ improves the agreement with the experimental masses of $B(2^+)$ and $B(1^+)$ mesons [28]. In Table XI the eigenvalues $M_0(1P)$ and $M_{\rm cog}(1P)$ together with $\Delta_{\rm SE}(1P)$ and $\Delta_{\rm str}(1P)$ are given.

In the field correlator method used in this paper, the mass difference between D_s and D (B_s and B) comes from two sources: (i) the self-energy difference (between light and s quarks), which is around 50 MeV; (ii) the difference in e.v.'s of the Dirac equation or spinless Salpeter equation for two different current masses, $m_1 \leq 7$ MeV and $m_1 = m_s$. An important fact is that if one takes the conventional mass, $m_s = m_s(2\text{ GeV}) = 90 \pm 10$ MeV, then the e.v. difference is only $\sim$10 MeV.

We have assumed that in those relativistic equations the current mass enters at a different (smaller) scale, $m_s(\mu_0 = r_0^{-1})$, where r_0 is a typical radius of a HL meson. As shown in [40] $m_s(r_0^{-1})$ can be directly extracted from the ratios of the pseudoscalar decay constants, $\frac{f_P(D_s)}{f_P(D)}$ and $\frac{f_P(B_s)}{f_P(B)}$, and the value $m_s(r_0^{-1}) = 190 \pm 20$ MeV provides good agreement with recent experimental data of CLEO discussed in [40].

TABLE X. The constituent masses ω_q and ω_b (in MeV) for the $B(1P)$ and $B_s(1P)$ mesons ($m_{u(d)} = 0$, $m_s = 200$ MeV, $m_b = 4780$ MeV).

	$B(1P)$ meson	$B_s(1P)$ meson
$\omega_q(1P)$	680	730
$\omega_b(1P)$	4836	4840
$\omega_{\rm red}$	598	634

TABLE XI. The masses M_0, $M_{\rm cog}(1P)$, and $\Delta_{\rm SE}(1P)$, $\Delta_{\rm str}(1P)$ (in GeV) for the B, B_s mesons ($m_s = 200$ MeV, $m_{u(d)} = 0$, $m_b = 4780$ MeV).

	$B(1P)$	$B_s(1P)$
$M_0(1P)$	5885	5925
$\Delta_{\rm SE}$	−126	−70
$\Delta_{\rm str}$	−27	−20
$M_{\rm cog}(1P)$	5.732	5.835

APPENDIX C: FINE-STRUCTURE SPLITTINGS

The FS interaction consists of the spin-orbit and tensor potentials, which in the general case [42,43] are expressed via the potentials $V_i(2)$ ($i = 1, 2, 3$) and the static potential $V_{\rm st}$,

$$\hat{V}_{\rm FS}(r) = \hat{V}_{\rm SO}(r) + \hat{V}_T(r), \tag{C1}$$

$$\hat{V}_{\rm SO}(r) = \mathbf{l}\left(\frac{\mathbf{s}_1}{2\omega_1^2} + \frac{\mathbf{s}_2}{2\omega_1^2}\right)\left(\frac{1}{r}\frac{dV_{\rm st}}{dr} + \frac{2}{r}\frac{dV_1}{dr}\right) + \boldsymbol{l}(\mathbf{s}_1 + \mathbf{s}_2)\frac{1}{\omega_1\omega_2}\frac{1}{r}\frac{dV_2}{dr}; \tag{C2}$$

$$\hat{V}_T(r) = \hat{S}_{12}\frac{V_3(r)}{4\omega_1\omega_2} \quad \text{with } \hat{S}_{12} = 3(\boldsymbol{\sigma}_1, \mathbf{r})(\boldsymbol{\sigma}_2\mathbf{r}) - \boldsymbol{\sigma}_1\boldsymbol{\sigma}_2. \tag{C3}$$

In QCD the static potential $V_{\rm st}(r)$ and the potentials $V_i(r)$ ($i = 1, 2, 3$) can be expressed via the field correlators (the vacuum average over the gluonic fields) [43]. In the general case each of these potentials can contain P and NP contributions.

The studies of the potentials $V_{\rm st}(r)$, $V_i(r)$ on the lattice and analytically in [42,43] have shown that in the static potential,

$$V_{\rm st}(r) = V_P(r) + S(r), \tag{C4}$$

both the vector P term $V_P(r)$ and NP scalar (confining) term $S(r)$ are equally important, while in $V_2(r)$ and $V_3(r)$ the P term dominates and in $V_1(r)$ the NP term dominates [44], i.e. $V_2(r) = V_{2P}(r)$, $V_3(r) = V_{3P}(r)$, $V_1(r) = V_{\rm NP}(r)$. Then, applying the Gromes relation [42],

$$\frac{dV_{\rm st}}{dr}+\frac{dV_1}{dr}=\frac{dV_2}{dr}, \tag{C5}$$

separately to vector and scalar potentials, in the considered approximation one obtains the relations

$$\frac{dV_P}{dr}=\frac{dV_2}{dr}; \qquad \frac{dS}{dr}=-\frac{dV_1}{dr}, \tag{C6}$$

which simplify the FS interaction.

After averaging over the radial w.f., the mass operator $\Delta M_{\rm FS}$, responsible for the FS splittings, can be presented in the form

$$\Delta M_{\rm FS}=\lambda_1 \boldsymbol{ls}_1+\lambda_2\boldsymbol{ls}_2+\frac{t}{4}\hat{S}_{12}. \tag{C7}$$

Here λ_1, λ_2, t are the matrix elements (numbers), universal for the chosen potential (C4):

$$\begin{aligned}\lambda_1(nP)&=\frac{1}{2\omega_1^2}A(nP)+\frac{T(nP)}{\omega_1\omega_2},\\ \lambda_2(nP)&=\frac{A(nP)}{2\omega_2^2}+\frac{T(nP)}{\omega_1\omega_2}, \qquad t(nP)=\frac{T(nP)}{\omega_1\omega_2},\end{aligned} \tag{C8}$$

with the m.e.

$$T(nP)=\left\langle\frac{V_P'}{r}\right\rangle_{nP}; \qquad A(nP)=\left\langle\frac{V_P'-S'}{r}\right\rangle_{nP}. \tag{C9}$$

To establish correspondence to heavy quarkonia, instead of λ_1, λ_2 it is more convenient to introduce the matrix element a, which defines the SO splitting:

$$a=\frac{1}{4}\left(\frac{1}{\omega_1^2}+\frac{1}{\omega_2^2}\right)A+t. \tag{C10}$$

To define the FS splittings of a HL meson, we follow here the approach developed in [30], where m.e.'s like $\langle \boldsymbol{ls}_1\rangle$, $\langle \boldsymbol{ls}_2\rangle$, $\langle S_{12}\rangle$ are calculated in the basis where j^2 is diagonal. Then the masses of the 2^+ state ($j=\frac{3}{2}$) and 0^+ state ($j=\frac{1}{2}$) can be written as

$$M(2^+)=M_{\rm cog}+a-0.1t, \tag{C11}$$

$$M(0^+)=M_{\rm cog}-2a-t, \tag{C12}$$

while the 1^+ states, with $|j=3/2\rangle$ and $|j=1/2\rangle$, are mixed. The mixing matrix can be expressed through the splittings a and t and the factor $\beta=\frac{A}{m_2^2}$ (we keep here the terms proportional to m_Q^{-2}):

$$\hat{O}_{\rm mix}=\begin{pmatrix} a-\frac{7}{6}t-\frac{2}{3}\beta & -\frac{\sqrt{2}}{6}(t+\beta)\\ -\frac{\sqrt{2}}{6}(t+\beta) & -2a+\frac{5}{3}t+\frac{2}{3}\beta\end{pmatrix}. \tag{C13}$$

In the HQ limit $\beta\to 0$, and our mixing matrix coincides with that from [30]. Then the eigenvalues and eigenvectors of this matrix define "higher" and "lower" masses M_H and M_L with $J^P=1^+$ and the decomposition of their w.f. The mass splittings are

$$M_H=M_{\rm cog}-\frac{1}{4}(2a-t)+\frac{1}{4}\sqrt{(2a-t)^2+32(a-t)^2}; \tag{C14}$$

$$M_L=M_{\rm cog}-\frac{1}{4}(2a-t)-\frac{1}{4}\sqrt{(2a-t)^2+32(a-t)^2}. \tag{C15}$$

Each of these levels is a decomposition of the $|j=\frac{3}{2}\rangle$ and $|j=\frac{1}{2}\rangle$ states. From (C13) it is evident that the weights in those decompositions depend only on the ratio $=\frac{a}{t}$. Only the value of this ratio defines the order of levels inside the nP multiplet, and for a given a/t the mixing angle ϕ in (9) can be easily calculated.

To interpret the tensor splitting t one can use the well-known P expression for the OGE interaction:

$$t(nP)=\frac{4}{3}\frac{\alpha_{\rm FS}\langle r^{-3}\rangle_{nP}}{\omega_q\omega_Q}. \tag{C16}$$

Then, for $\alpha_{\rm FS}=0.39$ one obtains the values $t\cong 12$ MeV for the B_s (B) mesons (with $\langle r^{-3}\rangle_{B_s}=0.080$ GeV^3, $\langle r^{-3}\rangle_B=0.0765$ GeV^3), which are close to those used in our analysis. For $D(1P)$ and $D_s(1P)$, a larger $\alpha_{\rm FS}=0.45$ is needed to have the value $t_D=t_{D_s}=34$ MeV ($\langle r^{-3}\rangle_D=0.052$ GeV^3 and $\langle r^{-3}\rangle_{D_s}=0.055$ GeV^3) used in our analysis.

Notice that the Coulomb-type order of levels, i.e. $M(0^+)<M(1_L^+)<M(1_H^+)<M(2^+)$, takes place only for the ratio $\frac{a}{t}\geq 0.60$. In our case this condition is satisfied and the level 1_H^+ lies below the 2^+ level; only this order of levels is observed in the $D(1P)$ multiplet, where the central value of the wide $1^{+'}$ level is smaller than the mass of the 2^+ state [26].

For negative $A<0$ and $a/t<0.60$, the level $1_H^{+'}$ lies above 2^+, i.e.

$$M_H(1^{+'})>M(2^+). \tag{C17}$$

[1] B. Aubert *et al.* (*BABAR* Collaboration), Phys. Rev. Lett. **90**, 242001 (2003).
[2] D. Besson *et al.* (CLEO Collaboration), Phys. Rev. D **68**, 032002 (2003); P. Krokovny *et al.* (Belle Collaboration), Phys. Rev. Lett. **91**, 262002 (2003).
[3] S. Godfrey and N. Isgur, Phys. Rev. D **32**, 189 (1985); S. Godfrey and R. Kokoski, Phys. Rev. D **43**, 1679 (1991).
[4] D. Ebert, V. O. Galkin, and R. N. Faustov, Phys. Rev. D **57**, 5663 (1998); **59**, 019902(E) (1998).
[5] S. Godfrey, Phys. Rev. D **72**, 054029 (2005).
[6] Yu. S. Kalashnikova, A. V. Nefediev, and Yu. A. Simonov, Phys. Rev. D **64**, 014037 (2001); Yu. S. Kalashnikova and A. V. Nefediev, Phys. Lett. B **492**, 91 (2000).
[7] R. Lewis and R. M. Woloshyn, Phys. Rev. D **62**, 114507 (2000); G. S. Bali, Phys. Rev. D **68**, 071501 (2003); A. Dougall *et al.*, Phys. Lett. B **569**, 41 (2003).
[8] Y. B. Dai, C. S. Huang, C. Liu, and S. L. Zhu, Phys. Rev. D **68**, 114011 (2003).
[9] S. Narison, Phys. Lett. B **605**, 319 (2005).
[10] M. Di Pierro and E. J. Eichten, Phys. Rev. D **64**, 114004 (2001).
[11] W. A. Bardeen, E. J. Eichten, and C. T. Hill, Phys. Rev. D **68**, 054024 (2003).
[12] K. D. Chao, Phys. Lett. B **599**, 43 (2004).
[13] E. S. Swanson, Phys. Rep. **429**, 243 (2006).
[14] P. Colangelo, F. De Fazio, and R. Ferrandes, Mod. Phys. Lett. A **19**, 2083 (2004); P. Colangelo and F. De Fazio, Phys. Lett. B **570**, 180 (2003); P. Colangelo, F. De Fazio, and R. Ferrandes, Nucl. Phys. B, Proc. Suppl. **163**, 177 (2007).
[15] E. van Beveren and G. Rupp, Phys. Rev. Lett. **91**, 012003 (2003); Mod. Phys. Lett. A **19**, 1949 (2004).
[16] D. S. Hwang and D. W. Kim, Phys. Lett. B **601**, 137 (2004).
[17] F. L. Wang, X. L. Chen, D. H. Lu, S. L. Zhu, and W. Z. Deng, High Energy Phys. Nucl. Phys. 30 (**2006**) 1041; Y. B. Dai, S. L. Zhu, and Y. B. Zuo, arXiv:hep-ph/0610327.
[18] Yu. A. Simonov and J. A. Tjon, Phys. Rev. D **70**, 114013 (2004).
[19] J. Vijande, A. Valcarse, and F. Fernandez, Phys. Rev. D **77**, 017501 (2008).
[20] Yu. A. Simonov, Phys. Rev. D **65**, 094018 (2002).
[21] S. Weinberg, Phys. Rev. Lett. **67**, 3473 (1991).
[22] J. L. Goity and W. Roberts, Phys. Rev. D **60**, 034001 (1999) and references therein; H. Georgi and A. Manohar, Nucl. Phys. **B234**, 189 (1984).
[23] Yu. A. Simonov, Phys. At. Nucl. **60**, 2069 (1997); Yu. A. Simonov and J. A. Tjon, Phys. Rev. D **62**, 014501 (2000); **62**, 094511 (2000).
[24] A. Yu. Dubin, A. B. Kaidalov, and Yu. A. Simonov, Phys. At. Nucl. **56**, 1795 (1993); Phys. Lett. B **323**, 41 (1994); E. Gubankova and A. Yu. Dubin, Phys. Lett. B **334**, 180 (1994).
[25] A. M. Badalian, B. L. G. Bakker, and Yu. A. Simonov, Phys. Rev. D **75**, 116001 (2007).
[26] W.-M. Yao *et al.*, Particle Data Group, J. Phys. G **32**, 1 (2006).
[27] V. M. Abazov *et al.* (D0 Collaboration), Phys. Rev. Lett. **99**, 172001 (2007).
[28] T. Aaltonen *et al.* (CDF Collaboration), Phys. Rev. Lett. **100**, 082001 (2008); R. K. Mommsen, Nucl. Phys. B, Proc. Suppl. **170**, 172 (2007); I. V. Gorelov, arXiv:hep-ex/0610080; P. Catastini, arXiv:hep-ex/0605051.
[29] F. K. Guo, S. Krewald, and U. G. Meissner, arXiv:0712 2953.
[30] R. N. Cahn and J. D. Jackson, Phys. Rev. D **68**, 037502 (2003).
[31] E. van Beveren and G. Rupp, Eur. Phys. J. C **32**, 493 (2004).
[32] O. Aquines *et al.* (CLEO Collaboration), Phys. Rev. Lett. **96**, 152001 (2006); G. Bonvicini *et al.* (CLEO Collaboration), Phys. Rev. Lett. **96**, 022002 (2006).
[33] A. M. Badalian and B. L. G. Bakker, Phys. Rev. D **62**, 094031 (2000); A. M. Badalian, B. L. G. Bakker, and V. L. Morgunov, Phys. Rev. D **60**, 116008 (1999).
[34] Y. Koma and M. Koma, Phys. Rev. Lett. **98**, 031601 (2007).
[35] A. M. Badalian, L. P. Kok, M. I. Polikarpov, and Yu. A. Simonov, Phys. Rep. **82**, 32 (1982).
[36] H. Feshbach, Ann. Phys. (N.Y.) **5**, 357 (1958).
[37] Yu. A. Simonov and M. A. Trusov, arXiv:hep-ph/0506058; arXiv:hep-ph/0607075.
[38] A. F. Falk and T. Mehen, Phys. Rev. D **53**, 231 (1996); P. L. Cho and M. B. Wise, Phys. Rev. D **49**, 6228 (1994).
[39] A. Zghiche (*BABAR* Collaboration), arXiv:0710.0314.
[40] A. M. Badalian and B. L. G. Bakker, arXiv:hep-ph/0702229; JETP Lett. **86**, 634 (2007).
[41] Yu. A. Simonov, Phys. Lett. B **515**, 137 (2001).
[42] E. Eichten and F. L. Feinberg, Phys. Rev. D **23**, 2724 (1981); D. Gromes, Z. Phys. C **26**, 401 (1984).
[43] A. M. Badalian and Yu. A. Simonov, Phys. At. Nucl. **59**, 2167 (1996).
[44] J. Pantaleone, R. H. Tye, and Y. J. Ng, Phys. Rev. D **33**, 777 (1986).